

Climate warming at European airports: human factors and infrastructure planning

Article

Published Version

Creative Commons: Attribution 4.0 (CC-BY)

Open Access

Williams, J. ORCID: <https://orcid.org/0000-0002-0680-0098>,
Williams, P. D. ORCID: <https://orcid.org/0000-0002-9713-9820>
and Venturini, M. (2026) Climate warming at European
airports: human factors and infrastructure planning.
Aerospace, 13 (2). 127. ISSN 2226-4310 doi:
10.3390/aerospace13020127 Available at
<https://centaur.reading.ac.uk/128427/>

It is advisable to refer to the publisher's version if you intend to cite from the work. See [Guidance on citing](#).

To link to this article DOI: <http://dx.doi.org/10.3390/aerospace13020127>

Publisher: MDPI

All outputs in CentAUR are protected by Intellectual Property Rights law,
including copyright law. Copyright and IPR is retained by the creators or other
copyright holders. Terms and conditions for use of this material are defined in
the [End User Agreement](#).

www.reading.ac.uk/centaur

CentAUR

Central Archive at the University of Reading

Reading's research outputs online

Article

Climate Warming at European Airports: Human Factors and Infrastructure Planning

Jonny Williams ^{1,*}, Paul D. Williams ¹ and Marco Venturini ²

¹ Department of Meteorology, University of Reading, Reading RG6 6ET, UK; p.d.williams@reading.ac.uk

² Amigo s.r.l., 00196 Rome, Italy

* Correspondence: j.h.t.williams@reading.ac.uk

Abstract

Temperature and related thermal comfort metrics at a representative 9-member ensemble of airports in Europe are presented using a combination of historical (1985–2014) and future projection (2035–2064) timescales under a variety of forcing scenarios. Data are shown for summer (June–July–August) and the nine sites are further grouped into ‘oceanic’, ‘continentally influenced’, and ‘Mediterranean coastal’ climate types, which ameliorates visualisation and provides more generalised policy-relevant results. Using the Humidex metric, it is shown that some airports in southern Europe may enter a ‘dangerous’ ($>45^{\circ}\text{C}$) regime of human discomfort. This would be accompanied by economic impacts related to longer mandated rest periods for ground workers, as well as increased water intake and changes to health and safety training. The coincidence of the 38°C flash point of kerosene jet fuel with perturbed daily maximum temperature occurrence thresholds at some sites will likely also have knock-on effects on safety practices since some sites may experience 70% of future summer days with temperatures exceeding this value. Using an 18°C threshold for defining cooling and heating ‘degree days’, increases in cooling requirements are projected to be larger than reductions in heating for continental and Mediterranean sites, and heatwave occurrence (3 or more days at or above the 95th historical percentile) may increase by a factor of 10. From a building and infrastructure services perspective, increased temperature variability around larger average values has the potential to reduce safe runway lifetimes and increase structural fatigue in large-span steel terminal buildings.

Keywords: temperature; comfort index; climate change; human factors

1. Introduction



Academic Editor: Miroslav Kelemen

Received: 19 December 2025

Revised: 18 January 2026

Accepted: 27 January 2026

Published: 28 January 2026

Copyright: © 2026 by the authors. Licensee MDPI, Basel, Switzerland. This article is an open access article distributed under the terms and conditions of the [Creative Commons Attribution \(CC BY\) license](https://creativecommons.org/licenses/by/4.0/).

Climate change is frequently referred to as a ‘wicked’ problem [1]; one which is “complex, interconnected, contradictory, located in an uncertain environment, and embedded in landscapes that are rapidly changing” [2]. In the context of aerospace, there are few areas which are untouched by it, whether one looks at route planning [3], auxiliary power unit energy usage [4] or even airport terminal design [5]. From a human factors point of view, airport ground workers (luggage, catering, marshallers) are subject to all weather conditions and are particularly susceptible to extremes of heat [6].

This work describes several metrics which are of particular interest to airport and aircraft operators and their staff. Firstly we discuss Humidex—a measure of human comfort combining temperature and humidity—before moving on to kerosene flash point exceedance, cooling and heating ‘degree days’, heatwaves, and finally temperature occurrence percentiles and extrema.

Aviation has been named as a key ‘vulnerable economic sector’ by the Intergovernmental Panel on Climate Change [7], and the potential health and safety effects on ground workers here are stark. For example, as well as the possibility of heat stroke explicitly included in Humidex, those working outside at the hottest sites will require longer breaks, higher water intake and training in how to recognise and mitigate deleterious health effects [8–10]. All of these impacts have a financial cost associated with them, and although it is not within the scope of this article to quantify them—the interested reader is referred to the work of Zhao et al. [11]—some of the numbers given in the study of Sun et al. [12] are sobering. For example, by 2060, global economic losses due to extreme heat may exceed 4% globally, depending on the effective emissions scenario experienced up to that date. The reasons for these losses relate to reduced productivity from increased human heat stress, as well as indirectly disrupted supply chains. Both of these effects have strong resonances with the aviation industry and to put this number in perspective, The International Air Transport Association (IATA) estimated that in 2023, the air transport industry contributed over GBP 100 billion in the UK alone (<https://www.iata.org/en/iata-repository/publications/economic-reports/the-value-of-air-transport-to-united-kingdom/> accessed 16 December 2025).

From a global building services perspective, the 2016 study of Hasegawa et al. [13] estimates that economic losses brought about by increased cooling demand will outweigh the gains due to reduced heating. They do, however, note that there remain significant socioeconomic and regional uncertainties affecting this balance, an aspect explored further by Lizana et al. [14], who discuss the challenges inherent to the uptake of sustainable cooling systems.

There are also structural considerations to be taken into account when maintaining and planning future airport infrastructure. For example, diurnal temperature ranges are increasing, which will exacerbate structural fatigue due to larger cycles of deformation (expansion/contraction) [15], and the absolute increase in overall temperatures due to global warming may reduce the integrity of wide-span steel structures due to expansion joint failures [16]. These structural aspects are not limited to buildings, however. Indeed, in 2022, the single-runway Luton airport near London suffered an extreme temperature-induced—38°—asphalt failure which caused significant (and costly) delays [17]. Concrete and ‘concrete-asphalt’ aggregate runways (‘pavements’) are similarly affected, with Barbi et al. [18] quoting a reduction in lifetime of up to 14 years due to climate change.

The remainder of this work is structured as follows: Section 2 details the specific background scientific and mathematical basis for the parameters of interest (each within their own Section); Section 3 is similarly split in accordance with the respective sections in Section 2; Section 3.6 provides a high-level summary table; Section 4 provides further discussion, gives our ‘take home’ conclusions, and indicates direction and motivation for future work. To close, Appendix A gives a first-order estimate of how evaporative cooling may impact the results shown in Section 3 if appropriately bias-corrected vector wind components become available.

2. Materials and Methods

In this study, we use bias-corrected, open-source climate model outputs containing temperature and humidity data to explore how the evolving climate landscape at European airports may change by mid-century (2035–2064), compared to a historical baseline (1985–2014). Previous studies using related methodologies applied to aircraft take-off performance [19] and near-airport noise pollution [20] have recently been published. These studies examined Newtonian force balance and community effects, respectively; the current study

focuses on the human factors of airport workers and passengers, as well as how temperature extremes could affect infrastructure planning.

The ten climate models used are taken from the database produced by the Coupled Model Intercomparison Project (version 6), CMIP6, which is organised under the auspices of the Intergovernmental Panel on Climate Change (IPCC) and the World Climate Research Programme (WCRP) [21]. The models span a wide range of climate sensitivity values (how much equilibrium warming results from a doubling of carbon dioxide), and their data is freely available from the Earth System Grid Federation (ESGF) [22]. The models are discussed in more detail in Williams et al. [19].

In order to quantify the level (i.e., the severity) of climate change going forward, we use Shared Socioeconomic Pathways (SSPs). The SSPs are split into ‘families’ which qualitatively describe the amount of climate change that can be expected. There are many different potential scenarios, and those considered here are shown in Table 1, and the interested reader is referred to the work of van Vuuren et al. [23] for detailed definitions and discussions.

Table 1. Shared Socioeconomic Pathways (SSPs) used; see van Vuuren et al. [23] for more details.

Scenario Name	Detail	Description
SSP1-2.6	‘Sustainable development’; $2.6 \text{ W}\cdot\text{m}^{-2}$ top of atmosphere forcing at 2100.	Low level of climate change
SSP3-7.0	‘Regional rivalry’; $7.0 \text{ W}\cdot\text{m}^{-2}$ top of atmosphere forcing at 2100.	Medium level of climate change
SSP5-8.5	‘Fossil-fuelled’ development; $8.5 \text{ W}\cdot\text{m}^{-2}$ top of atmosphere forcing at 2100.	High level of climate change

To assist in the interpretation of the data from a large number of airports, we reduce the number of sites shown in the following results section from 30—discussed in Williams et al. [20] and Williams et al. [19]—to 9. This reduction is achieved using *k*-means clustering on the 30-site ensemble to find 9 centroid locations [24]; the airports closest to each of these is then chosen. To further simplify analysis, the 9 sites are then grouped into 3 climate zones; ‘oceanic’, ‘continental influence’ and ‘Mediterranean coastal’. The oceanic sites broadly conform to the *Cfb* category of the Köppen climate classification system [25] and ‘Mediterranean coastal’ to the *Csa* category. The other sites in Figure 1 are more distant from the coast and hence have a degree of ‘continental’—Köppen classifications *Dfa* and *Dfb*—influence on their climate, such as wider temperature ranges. This is due to their ‘transitional’ locations between the more rigorously adhered-to climatic oceanic and Mediterranean regimes experienced by the other sites. Figure 1 and Table 2 detail these sites and regions.

The larger 30-site ensemble includes Europe’s 25 busiest [19], and hence the results shown here and in our previous studies are most applicable to major hub airports. From a geographical perspective, the remaining airports in the larger group of sites are largely in very close proximity to the coloured polygons shown in Figure 1, and hence the exact choice of the subset is likely to be small. That said, extending the analysis shown here—and in related studies—to explicitly include European Atlantic islands such as the Açores would provide additional policy-relevant insights.

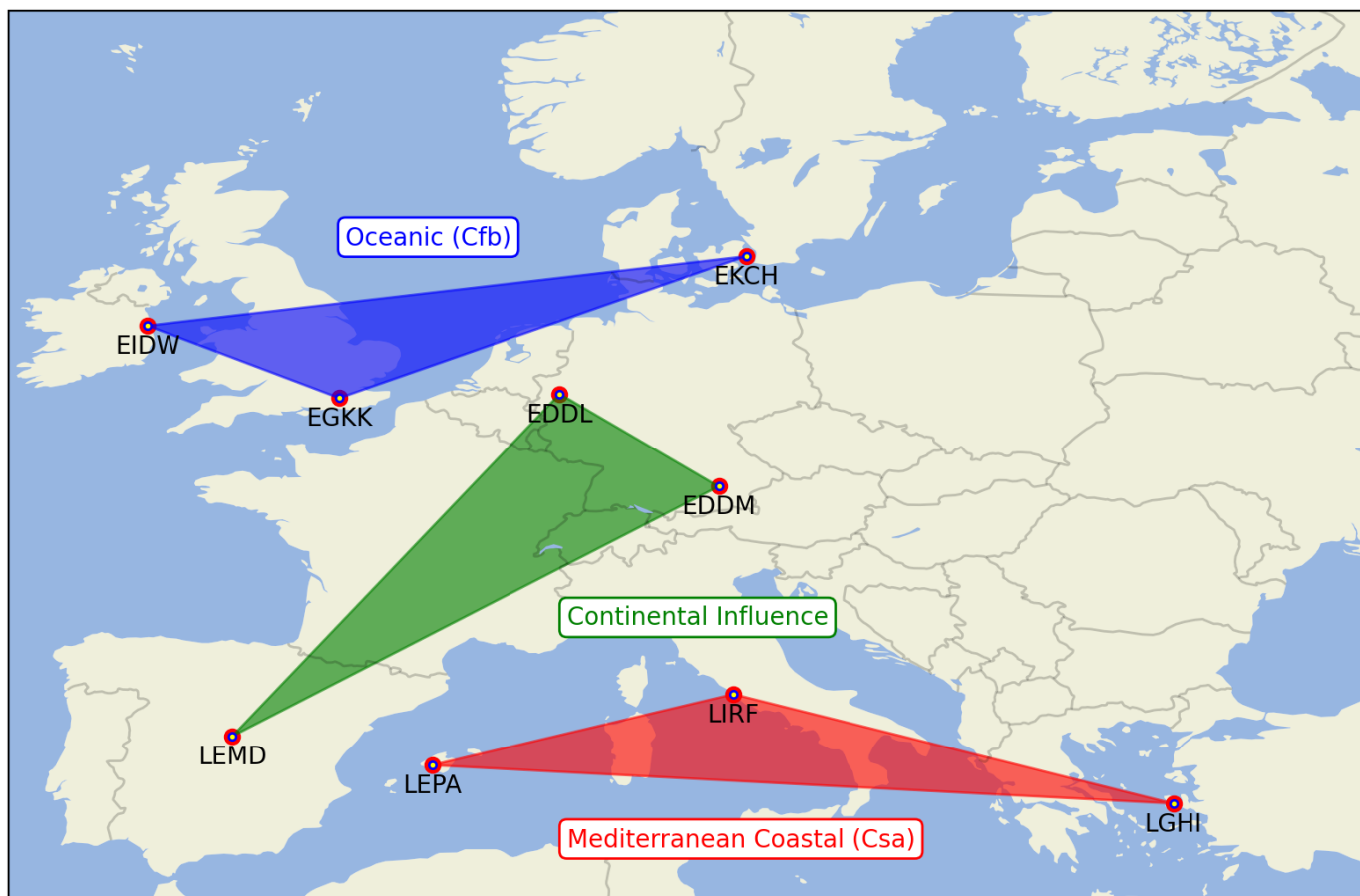


Figure 1. The subset of 9 airports was chosen to better visually represent the larger 30-airport ensemble. The blue region represents oceanically controlled sites, the green regions show those with a large continental influence, and the red region shows those of a coastal Mediterranean nature. Precise coordinates are given in Table 2.

Table 2. The subset of 9 airports used in the results figures below and shown in Figure 1.

Airport	ICAO Code	Climate Classification (Köppen)	Latitude, Longitude
Dublin	EIDW	Oceanic (Cfb)	53.4213°, -6.27007°
London Gatwick	EGKK	Oceanic (Cfb)	51.1481°, -0.19028°
Copenhagen Kastrup	EKCH	Oceanic (Cfb)	55.6179°, 12.656°
Düsseldorf	EDDL	Continental influence	51.2895°, 6.76678°
Munich	EDDM	Continental influence	48.3538°, 11.7861°
Madrid Barajas	LEMD	Continental influence	40.4936°, -3.56676°
Palma De Mallorca	LEPA	Mediterranean coastal (Csa)	39.5517°, 2.73881°
Rome (Fiumicino)	LIRF	Mediterranean coastal (Csa)	41.8045°, 12.2508°
Chios Island National	LGHI	Mediterranean coastal (Csa)	38.3432°, 26.1406°

Although it is not the purpose of this work to give a detailed literature review of available heat metrics, it should be mentioned that there are more than 100 indices of bioclimatic comfort [26]. These include the Wet Bulb Globe Temperature, WBGT [27] and the Universal Thermal Climate Index, UTCI [26]. The latter's evaporative cooling effect is discussed in Appendix A to contextualise the results shown below using the Humidex metric, which is discussed in detail in Section 2.1.

As well as the evaporative effect of wind discussed in Appendix A, some metrics also involve estimation of the increase in 'feels like' temperature due to solar radiation. A full

treatment of this would necessitate a detailed consideration of geometrical (latitude, solar zenith angle) and meteorological (cloud cover, air pollution) impacts. The inclusion of the former is not unambiguous since it depends on, e.g., surrounding mountains, and a full treatment of the latter's uncertainties lies out of the scope of the present work—see Chesnoiu et al. [28] for a recent model study discussing this in detail. Therefore, at the current stage in this work, we do not include wind-induced cooling due to data availability and neglect solar radiative effects due to the large concomitant uncertainties that would be introduced thereby. The inclusion of both of these effects in future studies is strongly encouraged, however, since this will—in time—provide more nuanced conclusions.

2.1. Humidex

Humidex is one of the most widely used ways of quantifying human comfort levels. It was introduced in Canada in 1965 using the Fahrenheit scale and was reformulated in 1979 to use Celsius [29]. It is an empirical measure, albeit one founded upon physical principles. Essentially the Humidex value is the sum of the dry bulb temperature and a function of the vapour pressure, e , which is itself a function of the pressure and specific humidity. An illustration of the effect of specific humidity on Humidex is shown in Figure 2, which shows that under extreme conditions, the effect of humidity on dry bulb temperature can exceed 6°.

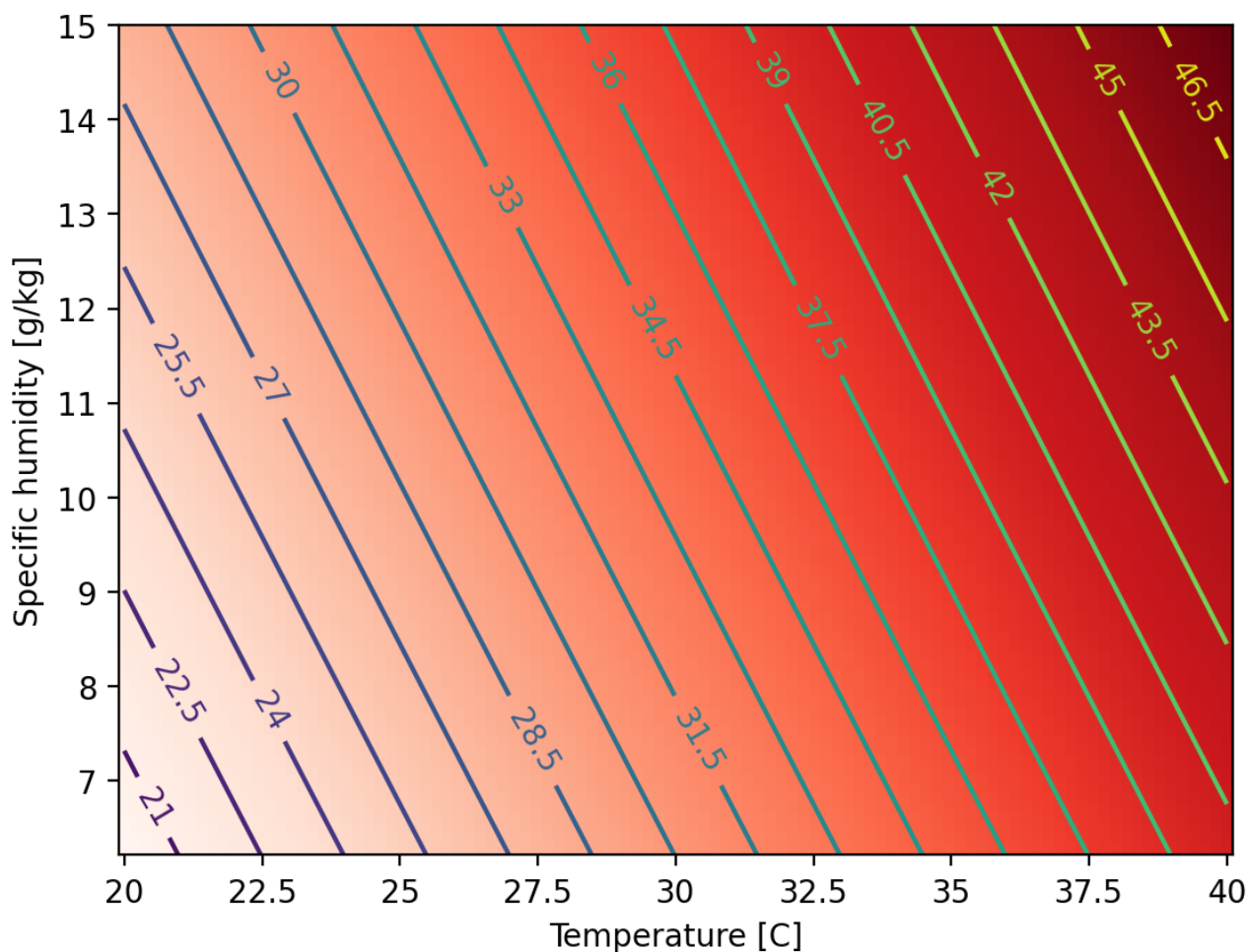


Figure 2. A representative illustration of Humidex (in degrees Celsius) as a function of dry bulb temperature and specific humidity. The vapour pressure is calculated using Equation (1) and a pressure of 1015 hPa. In extreme conditions (i.e., high temperature and humidity), the difference between the dry bulb temperature and that due to water vapour can exceed 6°.

Therefore we can straightforwardly construct climatologies of Humidex and hence provide information and guidance on future heat stress for ground workers across Europe. Crucially, these are traceable to previously published studies and hence provide a holistic human- and physical-factors assessment of how climate change could impact airport operations in the coming decades.

Vapour pressure e is calculated using

$$e = \frac{qP}{\epsilon + q}, \quad (1)$$

where q is specific humidity, P is pressure, and ϵ is the ratio of the molecular weights of water and dry air [30],

$$\epsilon = \frac{M_W}{M_d} \approx 0.622. \quad (2)$$

Humidex, H is defined by

$$H := T + \frac{5}{9}(e - 10), \quad (3)$$

or equivalently,

$$H := T + T_h, \quad (4)$$

where T_h is the apparent additional temperature experienced due to atmospheric water vapour content, which converts the vapour pressure's humidity effect to an equivalent 'feels like' temperature equivalent when $e > 10$. Humidex is not a thermodynamically derived 'physical' quantity but rather an empirical way of defining an additional heat stress load (hence the use of $:=$ rather than $=$ in Equation (3)). Rigorously, T_h could be negative under certain conditions but this is outside the scope of what Humidex was designed to represent. Additionally, even for the most northerly site in our ensemble, less than 1% of summer days exhibit daily mean e values below 10 hPa in the past historical period when averaged across all models.

Table 3 shows the qualitative definitions of different Humidex levels from the Canadian Centre for Occupational Health and Safety—https://www.ccohs.ca/oshanswers/phys_agents/humidex.html (accessed on 28 January 2026).

Table 3. Qualitative Humidex level descriptions. Note that in the calculations below, we ensure that the levels are contiguous with the boundaries at 30, 40 and 45 °C.

Humidex Range [°C]	Degree of Comfort
20–29	Little discomfort
30–39	Some discomfort
40–45	Great discomfort; avoid exertion
46 and over	Dangerous; heat stroke possible

2.2. Kerosene Flash Point Exceedance

A flammable liquid's 'flash point' is defined as the "lowest liquid temperature at which, under certain standardised conditions, a liquid gives off vapours in a quantity such as to be capable of forming an ignitable vapour/air mixture" [31]. This should not be confused with the auto-ignition or 'spontaneous combustion' temperature, which is much higher. For example, for standard jet fuel kerosene, the flash point is 38 °C and the auto-ignition temperature is 210 °C. These numbers depend on various physical and chemical factors but for the purposes of this study, we assume that the flash point of kerosene is a constant 38 °C. This enables us to provide unambiguous quantification of the risk of flash

point exceedance at European airports and how this may change in the future under certain assumptions concerning future climate change pathways.

We emphasise here that exceedance of this 38 °C threshold does not mean ignition will occur; of course this temperature is regularly exceeded already in parts of Europe with no deleterious effects. It does, however, provide a pertinent orientation for climate change studies and illustrates how some health and human safety considerations—previously confined to lower latitudes—should be taken into account more widely going forward.

2.3. Cooling and Heating Degree Days

Cooling and heating degree days (CDD, HDD) are representative of the amount of power used in the control of temperature and are widely used in the fields of domestic power requirements [32], building design [33], and climate change assessments [34].

CDD is defined as the cumulative residual of the temperature for a given day with respect to a given threshold value. It has a limiting lower value of zero. Mathematically, this can be written

$$CDD = \begin{cases} T_C - T_{\text{threshold}}, & \text{if } T_C > T_{\text{threshold}} \\ 0, & \text{otherwise.} \end{cases} \quad (5)$$

where T_C is the temperature in degrees Celsius and $T_{\text{threshold}}$ is the threshold temperature. In this work we use $T_{\text{threshold}} = 18$ °C which is a widely used value in the literature [35].

Equivalently, the calculation for HDD is

$$HDD = \begin{cases} T_{\text{threshold}} - T_C, & \text{if } T_C < T_{\text{threshold}} \\ 0, & \text{otherwise.} \end{cases} \quad (6)$$

Although HDD and CDD are physically 'equivalent' in their symmetry around $T_{\text{threshold}}$, this does not mean that the costs associated with altered heating or cooling are too. This will depend on numerous features of the heating, ventilation and air conditioning—HVAC—systems, which are outside the scope of this work. That said, previous work does imply that increases to CDD are likely to outweigh those of the decreasing HDD, albeit with significant uncertainties [36].

2.4. Heatwaves

The term "heatwave" does not have an unambiguous physical definition, although there are two key factors common to essentially all definitions: an exceedance threshold and a period over which the threshold is exceeded. In this work we use the 95th percentile for the former and 3 days for the latter, which are in line with many previous studies [37]. For a review of methods and definitions see Bunting et al. [38].

This extensive review also makes the crucial point—explored in the section of this work on the Humidex comfort index—that often heatwaves are discussed purely as a physical phenomenon. They state that they "see little to no usage of non-climatological variables such as exposure, vulnerability, population, and land cover/land use". There are of course studies which actually purely concentrate on these 'human factors', however we assert that these facets of the effect of a changing temperature landscape are significantly under-represented in the wider climate change literature, particularly when addressing aviation-specific challenges.

Examples of the 'hidden' impacts of increasing temperature and occurrence frequency of heatwaves include thermally induced degradation of kidney health [39], sleep disrup-

tion [40] and increased incidence of workplace accidents due to increased frequency of extreme heat [41].

2.5. Temperature Occurrence Percentiles and Extrema

The changing nature of temperature distributions under climate change has been the subject of many studies (see Molina et al. [42] for a recent, area-aggregated study), and indeed this has already been discussed summarily for this data set elsewhere [19].

After accounting for changes to the mean temperature expected under different climate forcing scenarios, if two distributions of daily temperature values are distributed equally, then histograms (or their continuum analogue, the Gaussian kernel density estimate, KDE) of their binned occurrence frequencies will be identical. This is mathematically equivalent to an identity line ($y = x$) in a plot of the percentiles of each distribution, often referred to as a ' $Q - Q'$ plot.

Examination of these complementary plots can show us not only how extreme hot days may change in their frequency going forward but also how the overall range of temperatures may evolve as well. This latter metric has important and frequently overlooked building services [43] and runway maintenance [44] consequences.

3. Results

3.1. Humidex

Figure 3 shows the distribution of Humidex levels and how they change with different levels of forcing. It also shows the comfort levels defined in Table 3. Clearly there is a large historical range associated with the geographical spread of the sites used. It ranges from around 20 °C for Dublin (EIDW) to as high as ≈ 34 °C for Rome.

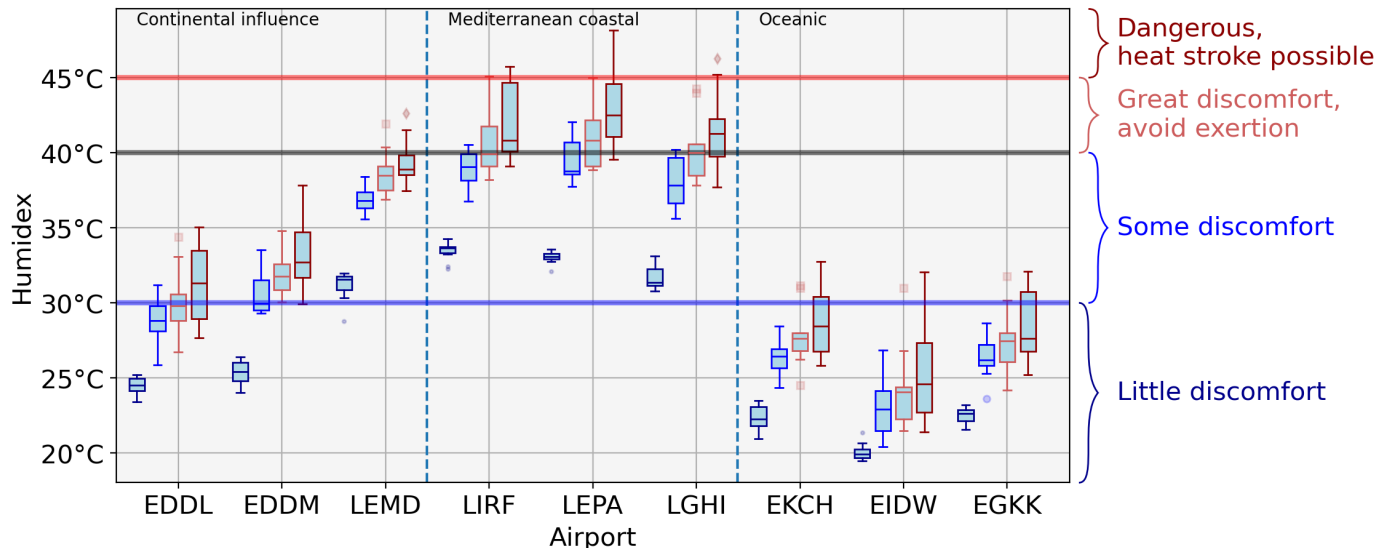


Figure 3. Box-and-whisker plots of Humidex, H , for each of the airports shown in Figure 1 and for each SSP scenario. The coloured horizontal lines and the text on the right hand-side illustrate the pre-defined levels of comfort shown in Table 3. The three climate regimes are shown, separated by vertical dashed lines.

In the historical period, all but one of the oceanic and continentally influenced sites lie firmly within the lowest 'little discomfort' category. All three Mediterranean sites exhibit 'some discomfort' historically, as does Madrid, which has elevated temperatures driven by its southern latitude compared to Düsseldorf and Munich. The variability of the models in the historical period is also smaller than for the future projections, which is the expected

behaviour since the models themselves are tuned to reproduce historical temperature trends before being run into the future. A detailed discussion of tuning processes can be found in Hourdin et al. [45].

Turning our attention to the future projections, it is notable that in all cases considered in Figure 3, the difference between the historical and SSP results for each site is smaller than the differences between each of the SSPs. This is particularly the case for the Mediterranean and continental influenced sites, where this difference is typically above 5 °C and as high as 10 °C. Putting this in terms of perturbations to the qualitative Humidex categories for each site, there is a general shift from what we term ‘category N ’ to ‘category $N + 1$ ’ as forcing is increased to its maximum. What we mean by this is that a state of ‘little discomfort’ shifts up to ‘some discomfort’, and so forth. However, since the width of the ‘some discomfort’ category is 10 °C and that of the ‘great discomfort’ category is only 5 °C, the categorical increases for the Mediterranean sites are more pronounced, with some outlier models giving shifts from levels of ‘some discomfort’ to ‘dangerous’ conditions where heat stroke is possible.

3.2. Kerosene Flash Point Exceedance

Figure 4 shows the probability of daily JJA maximum temperatures exceeding the flash point of kerosene, 38 °C.

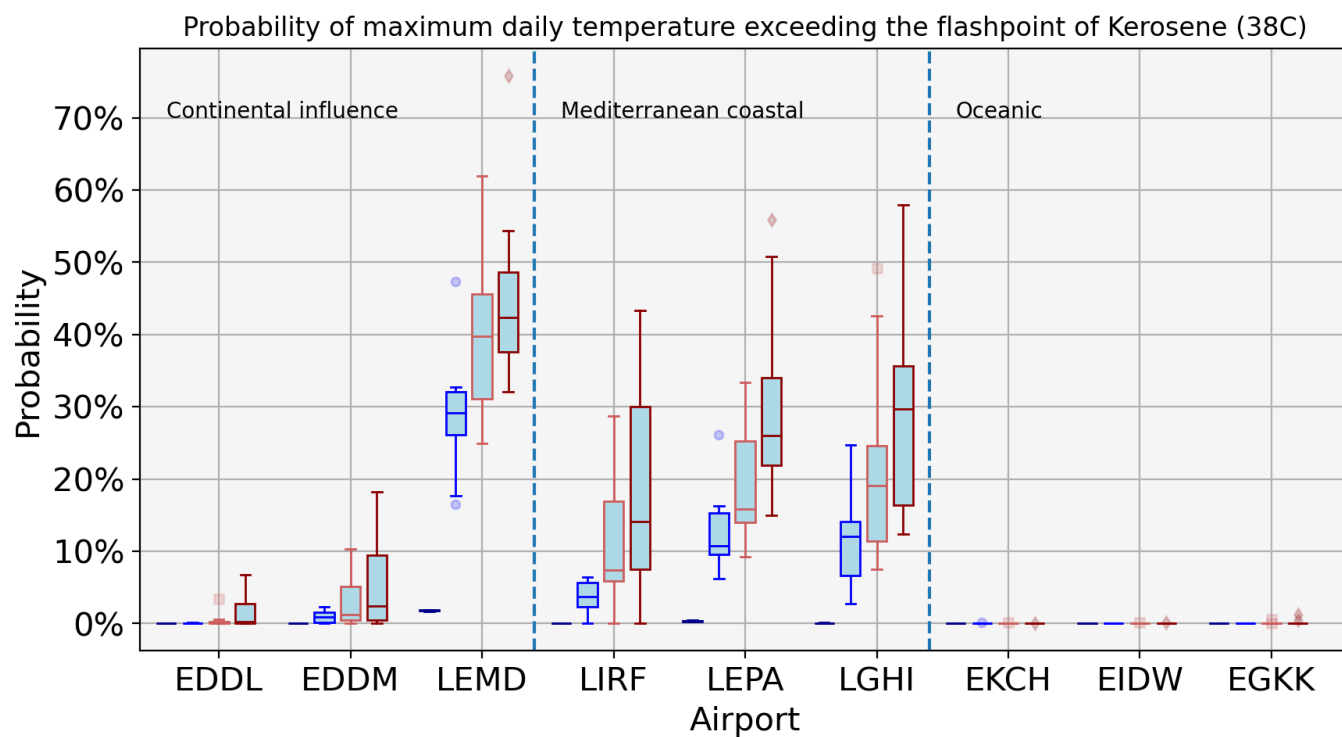


Figure 4. Probability of maximum daily JJA temperature exceeding the flash point of kerosene. The box and whisker plots show the intra-ensemble variability, and the historical, SSP1, 3 and 5 results are shown in dark blue, blue, red, and dark red, respectively. The three climate regimes are shown, separated by vertical dashed lines.

What is immediately clear from Figure 4 is that the probabilities are zero or, at maximum, $\approx 2\%$ for Madrid and that they significantly increase with future forcing. Interestingly, the values for the oceanic airports remain at zero with the exception of some outliers at London Gatwick (EGKK). This potentially points to an underestimation of future warming given that parts of England experienced temperatures of over 40 °C in July 2022 [46].

In extreme cases, numbers as high as 70% may be expected for SSP5-8.5 conditions, and over 30% for SSP1-2.6. This most optimistic SSP considered in this work is broadly

equivalent to a global mean increase of 2° by 2100 with respect to preindustrial conditions [47]. For reference, we are already in a ‘1.5 degree’ world, with 2024 being the first year where the global mean temperature exceeded this threshold [48].

As discussed above in Section 2.2, this does not mean that actual ignition rates under already-mandated storage conditions will increase, but it unambiguously illustrates the changing health and safety landscape. For airports in our site ensemble which are projected to have a non-zero number of days above 38°C where they previously had none, fuel handling and storage guidelines will likely need revisiting.

3.3. Heating and Cooling Degree Days

Figures 5 and 6 show changes to heating and cooling degree days, respectively.

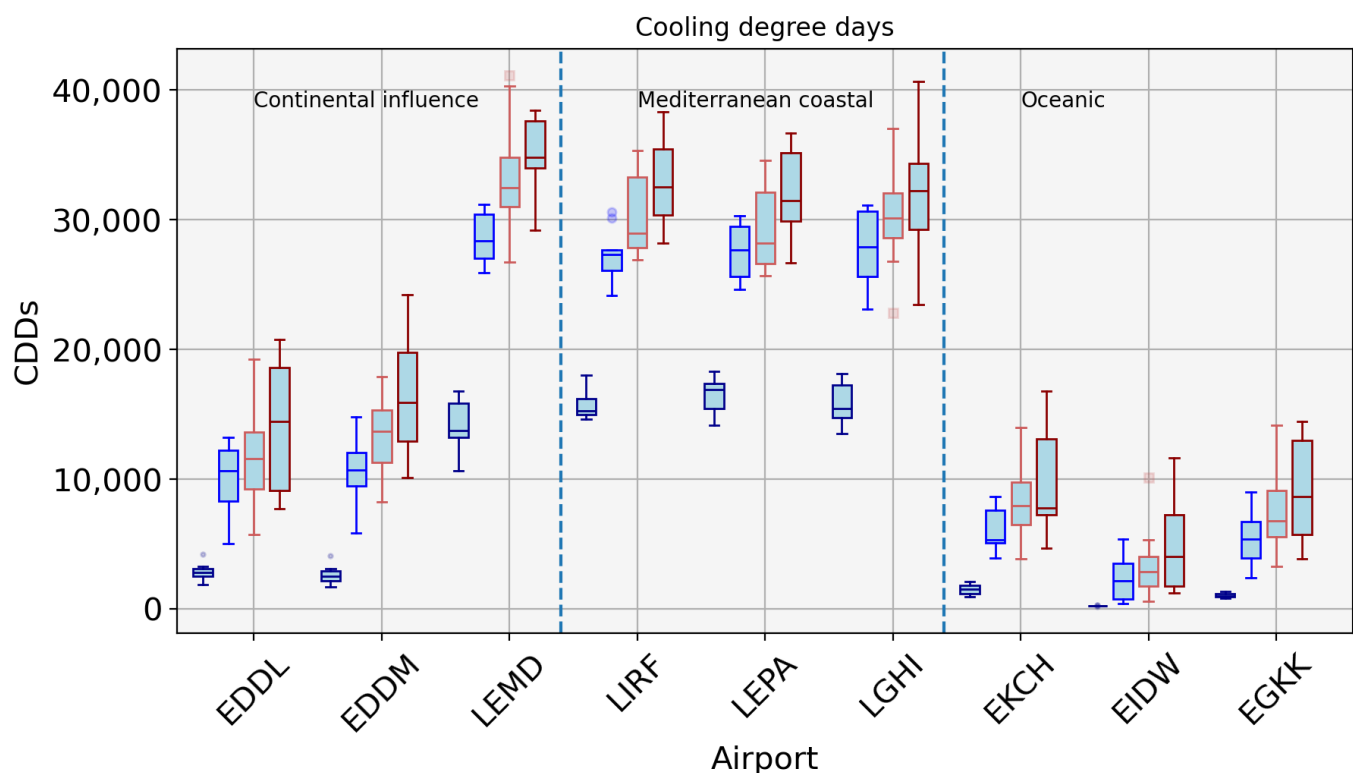


Figure 5. Number of cooling degree days for each SSP. The box and whisker plots show the intra-ensemble variability, and the historical, SSP1, 3 and 5 results are shown in dark blue, blue, red, and dark red, respectively. The three climate regimes are shown, separated by vertical dashed lines.

In Figure 5, the inter-model spread is large meaning that, although the median values do increase monotonically for each site shown, the ‘whiskers’ of the difference SSP estimates mutually overlap. This is not to say that the distributions are statistically indistinguishable from one another, but it does indicate the potential difficulties in infrastructure planning for different amounts of future climate forcing. As expected, the CDD count is lowest for the oceanic climate group; this is due to their lowest base temperature.

The site with the highest demand for cooling is Madrid, and this should be contrasted with the fact that this does not correspond to the site with the highest Humidex values, Figure 3. This not only illustrates the subtleties between changing estimates of temperature and heat stress inside and outside terminal buildings, but also emphasises the need to take humidity into account when assessing and dealing with the future changes to ambient climate for the benefit of airport workers and users.

Although CDDs are a widely used and easily calculated proxy for cooling energy demand, in general the relationship is non-linear and does not take latent heat (humidity) processes into

account, although techniques are available to quantify and account for these effects [49]. In this work, we do not incorporate latent heat effects but this could be performed in future work by, for example, using wet bulb globe temperature—WBGT—as in the 2021 study of Cao et al. [50]

We now turn our attention to the complementary measure of heating degree days—HDDs—in Figure 6.

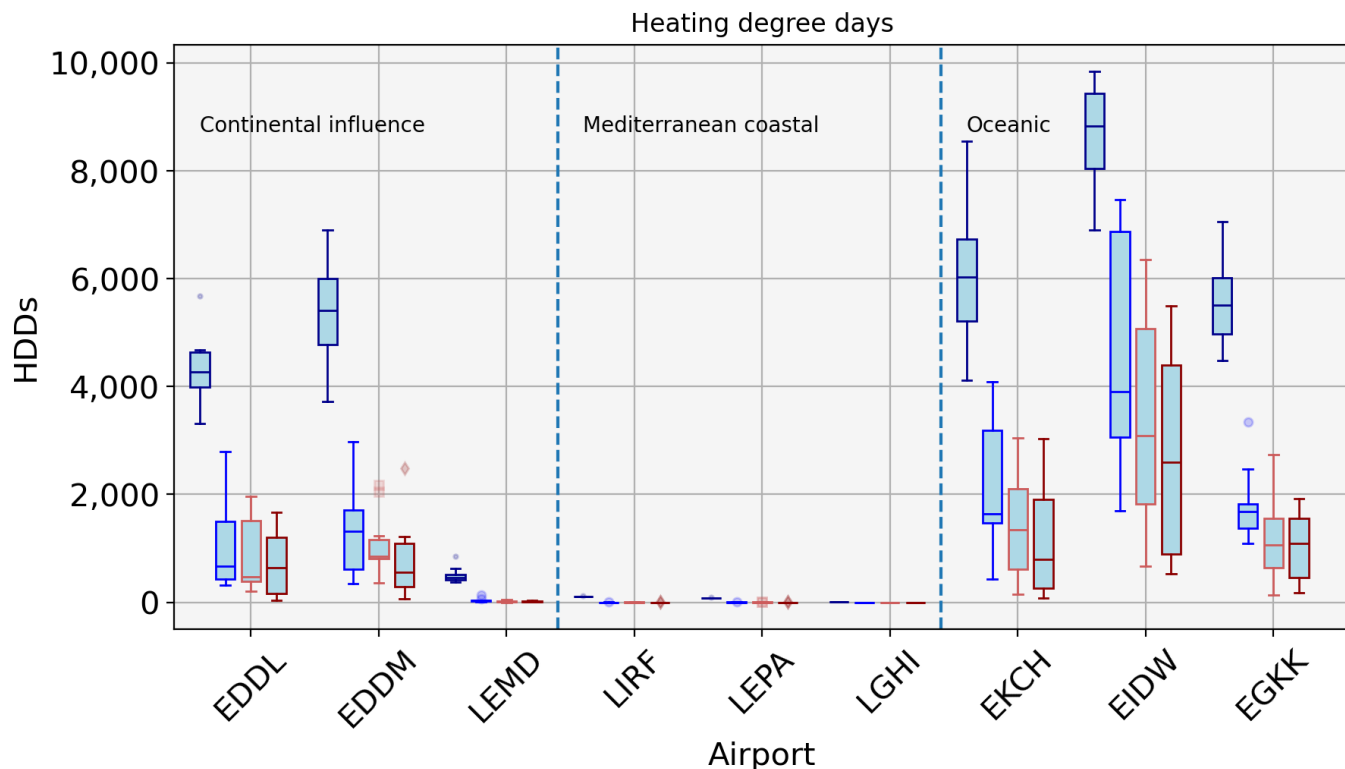


Figure 6. Heating degree days for each SSP. The box and whisker plots show the intra-ensemble variability, and the historical, SSP1, 3 and 5 results are shown in dark blue, blue, red, and dark red, respectively. The three climate regimes are shown, separated by vertical dashed lines.

The first thing to note about the numbers of HDDs contrasted with CDDs is that they are considerably smaller for the continental and Mediterranean groups: up to $\approx 40,000$ compared with $\approx 10,000$. This is not the case for the oceanic group, however, where the overall magnitudes of HDDs and CDDs are comparable. The reason for this is that a threshold temperature of 18°C is used in our calculations. This is a commonly used benchmark in ‘degree day’ studies—see, e.g., [51]—and the larger magnitude of the CDDs is due to the overall predominance of days well above this value in southern Europe. We will return to the concept of changing temperature distributions in the later section on ‘ $Q - Q'$ plots.

The HDDs are small in number even in the historical case for the Mediterranean sites, becoming negligible even with relatively small future forcing. This is broadly also the case for Madrid, whereas the other continental and all the oceanic sites retain the significant numbers of HDDs.

This study is restricted to the northern hemisphere summer (June–July–August), which explains much of the asymmetry in the magnitudes of the CDD and HDD distributions and we encourage future work to examine the equivalent changes expected for winter as well as a detailed economic evaluation. For example, when considering large, varied areas such as Europe, it is pertinent to assess whether the energy demand increase for cooling will be outweighed by a decrease in heating costs. Certainly for the oceanic regions shown here,

the changes shown are comparable in magnitude, albeit due to the fact that their summer mean temperatures are closer to 18 °C than the other regions.

3.4. Heatwaves

Figure 6 shows heatwave occurrences for the historical and SSP projections, which also includes the 1985–2014 JJA heatwave occurrence from the Central England Temperature—CET—record [52]. This additional observational record is shown to confirm the ability of the historical models’ results to reproduce the observed record from an arbitrary yet long-established European data set. More details regarding the historical and pre-industrial climatologies of each of the models are given in the references in Table A3 in Williams et al. [19].

Figure 7 clearly shows the expected increase in heatwaves for the SSPs; expected since we are defining heatwaves here with respect to the historical 95th percentile. In some cases the number of heatwaves may increase from around one every two years (summers) to as high as five per summer, a ten-fold increase. We examine the distribution of the temperatures with respect to their respective means in Section 3.5.

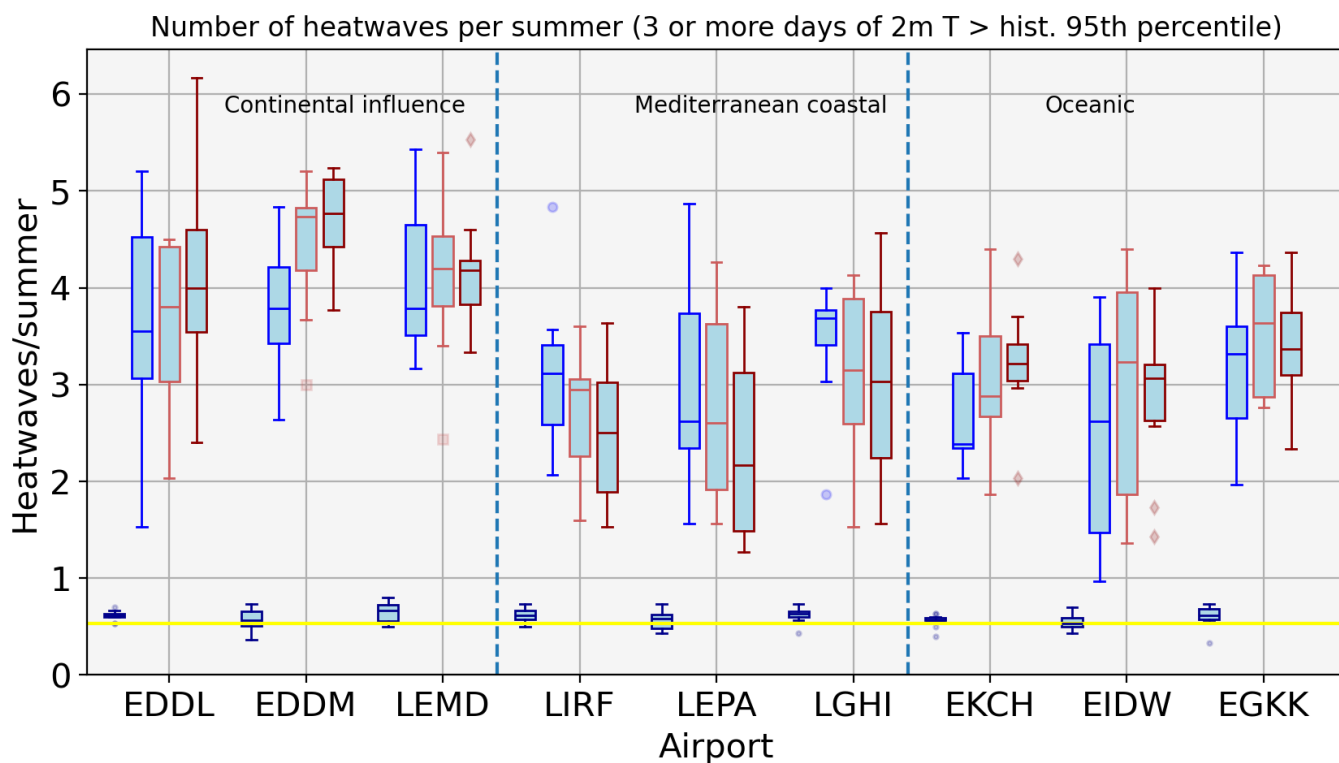


Figure 7. The number of heatwaves experienced by each site, where a heatwave is defined as a 3-or-more-day period of daily mean 2 m temperatures exceeding the 95th percentile of the historical simulations for each model, respectively. The box and whisker plots show the intra-model ensemble variability, and the historical SSP1, 3 and 5 results are shown in dark blue, blue, red, and dark red, respectively. The three climate regimes are shown, separated by vertical dashed lines, and the yellow horizontal line is the 1985–2014 JJA heatwave occurrence from the Central England Temperature data set.

Using this definition, the median number of heatwaves generally increases with forcing, although the inter-model spread is significant. Notably however—Indeed for all the Mediterranean sites—although the distributions have significant overlap, their median values actually *decrease* when forcing is increased from SSP1 to SSP3 and from SSP3 to SSP5 (Dublin and London Gatwick show mixed behaviour). Ostensibly this is a rather

surprising and counterintuitive result and points to underlying changes to the distribution of daily temperatures in addition to the overall increasing average. The highest number of heatwaves are projected to occur in continentally influenced sites, and this is attributed to the lower heat capacity of land versus ocean regions.

The next and final results section of this work examines this in more detail, firstly by taking the changing average into account and secondly by considering a continuum of thresholds, Q .

3.5. Temperature Occurrence Percentiles and Extrema

Figure 8 (a–i) show percentile–percentile ($Q - Q'$) plots of the nine sites, and (j) and (k) show Gaussian kernel density estimator plots for Madrid and London Gatwick, respectively.

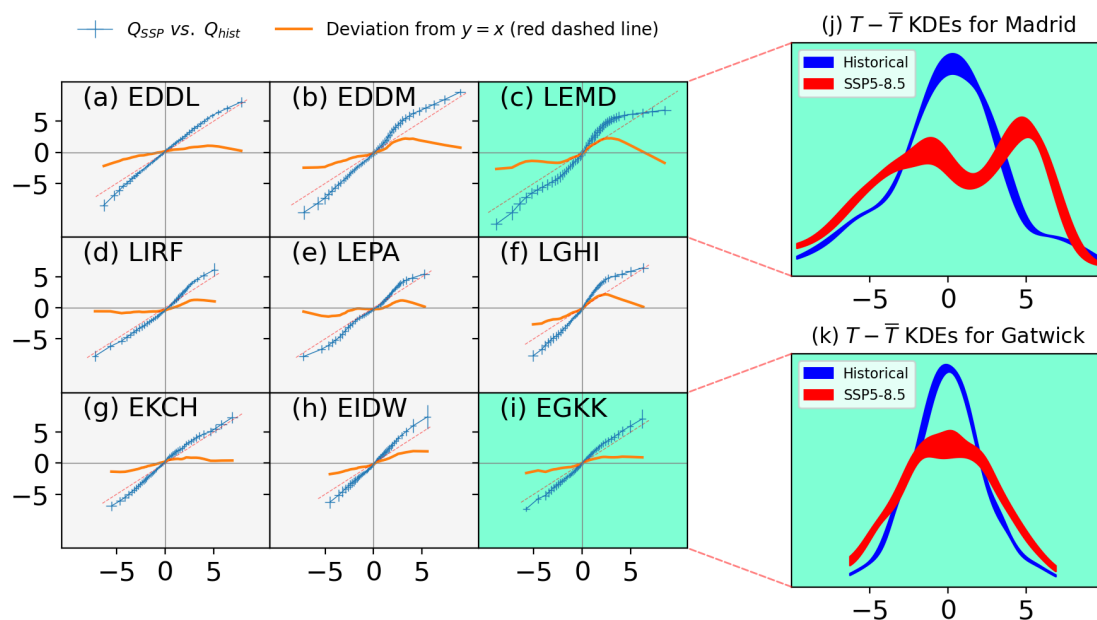


Figure 8. (a–i) $Q - Q'$ (percentile–percentile) plots are shown by the blue ‘plus’ symbols, where the extents of the arms in each axial direction show the respective inter-model spread. The historical data is on the x -axis and the y -axis shows the SSP5-8.5 results. The diagonal line ($y = x$) shows the line that would be made by the $Q - Q'$ plots if the distributions were identical. The solid line is the deviation from the $y = x$ line on the same y -axis scale. (a–c) are continentally influenced; (d–f) are Mediterranean coastal; (g–i) are oceanic. Note that the green lines in (c) and (i) indicate large and small amounts of deviation from $y = x$, respectively; (j,k) show the Gaussian kernel density estimate distributions and associated standard errors. The x -axis ranges of the KDE plots are chosen to match the historical Q ranges in (c) and (i), respectively.

In order to calculate the quantities used in Figure 8, the mean of each time series was subtracted, thus isolating the effect of the changing underlying distribution of temperature residuals. The Q values were then calculated for integer values from 1 to 100 and are shown as the blue ‘plus’ signs whose extents show the inter-model spread in each direction. To maximise signal to noise only the SSP5-8.5 results are shown.

For some of the sites shown in Figure 8, the $Q - Q'$ lines are near-linear ($y \sim x$)—such as that of London Gatwick, EGKK—and some deviate significantly—e.g., Madrid, LEMD. The Gaussian KDEs—with bandwidths calculated using the Scott’s rule implementation in SciPy—for these two sites are shown in the additional axes indicated with dashed lines. For Gatwick, the shape of the distributions is broadly uniform in the sense that the historical and SSP5-8.5 data are unimodal—they exhibit a single, well-defined peak value—and monotonically decrease away from the centre, where $T - \bar{T} \approx 0$ in this case.

This quasi-Normal (i.e., Gaussian) distribution is also evident in the historical distribution for Madrid, albeit with noticeable ‘shoulders’ around ± 5 °C, which are absent for Gatwick. However, the SSP5-8.5 distribution has several important and visually striking differences. Firstly, the red distribution in Figure 8(j) is bimodal, exhibiting two distinct KDE peaks around -1 °C and $+5$ °C, respectively. Secondly—and indeed causally linked to the first point—the width of the distribution is considerably wider for SSP5-8.5 than in the historical case (this is also the case for Gatwick, but to a reduced extent).

The reason for the appearance of bimodality in the SSP5-8.5 response for Madrid, whilst being absent for Gatwick, may be due to the different coupling regimes between the atmosphere and land surface in the two locations. In hot, inland situations, there will be a sharp perturbation in the balance between sensible and latent heat as surface soil moisture tends to zero, i.e., under summer temperature extremes—see, e.g., Seneviratne et al. [53]. Prevailing air mass and circulation changes may also play a role in this distributional change; however, we recommend that a full investigation of these underlying statistical effects be reserved for future studies.

These changes to underlying temperature distributions have wide implications and are well-studied in the wider climate change literature. These include studies of ‘compound’ (day–night) heatwaves [54], effects of extreme heat on electrical installations [55], reliability of structural elements [56] and socio-environmental effects on uses of alternative modes of transportation [57].

3.6. Summary Table

Table 4 shows brief policy-relevant summaries of the high-level messages from this study.

Table 4. Summary table of policy and stakeholder-relevant metrics.

Quantity	Summary
Humidex	All sites show qualitative ‘categorical’ changes; e.g., from ‘some’ to ‘great’ discomfort. Mediterranean sites may exhibit ‘dangerously’ hot conditions for ground workers.
Kerosene flash point exceedance	Some Mediterranean and continentally influenced sites may exhibit daily maximum temperatures exceeding 38 °C on more than half of summer days.
Degree days	The number of cooling degree days is up to approximately 4 times larger than heating ones for continental sites, and comparable for oceanic ones. Mediterranean sites exhibit negligible numbers of heating days even under historical conditions.
Heatwaves	Occurrences increase markedly, approaching 10 times that observed historically. The future absolute number of heatwaves is broadly independent of the site considered, although the numbers are higher for continental sites.

4. Discussion and Conclusions

Climate change is already having measurable negative effects on the airline industry, and these effects are projected to grow even with significant ongoing mitigation. These include degraded take-off performance—increases to take-off distance required and reductions in maximum mass load capacity—and increased exposure to noise pollution. Indeed, these are just two specific examples of many, with others including increased turbulence [58] and changing contrail properties [59].

In this vein we have performed a comprehensive review of the projected temperature and thermal comfort landscape for mid-century at European airports in summer compared to a historical baseline. We have used a regionally coarse-grained, nine-member ensemble, further grouped into three climate regimes: ‘Mediterranean coastal’, ‘oceanic’, and ‘con-

tinental influence'. This dimensional reduction will facilitate regional policymaking and stakeholder engagement, and we encourage future research using this simplified vision of climate change at European airports going forward. Indeed, although our conclusions are based on state-of-the-art climate model data—themselves based on complex physical and mathematical laws—our target engagement audience is wide and varied, including airport operators and regulators as well as atmospheric scientists.

There are many different ways of quantifying human thermal comfort, and we have used Humidex in our calculations due to the relative ease of its calculation, wide community uptake, and data availability reasons. Humidex is projected to increase significantly, particularly for the Mediterranean. Some southern European sites are projected to experience potentially 'dangerous' ($>45^{\circ}\text{C}$) levels of thermal discomfort under extreme warming conditions, and all sites become less comfortable to work in, for example, moving from states of 'little discomfort' to 'some discomfort'. Some extreme median value increases—say for Pantelleria—may approach 10°C .

Considering dry bulb temperatures—the temperature as shown by an 'everyday' thermometer—the conjunction of projected daily maximum temperature thresholds with the flash point of kerosene (38°C) is an unfortunate coincidence in terms of health, safety and environmental management. Above the flash point, sustained combustion *can* occur given the right containment and ignition conditions and therefore presents some evolving challenges for the European aviation sector. Airports in continental influenced and Mediterranean climates universally transition from negligible numbers (at most $\approx 2\%$ for Madrid) of summer days exceeding this threshold to—in extreme cases—approaching 70%. For oceanic climates, the probability remains in low single figures; however, it must be borne in mind that 40°C days have already occurred in the UK, lending credence to even the highest temperatures in the climate model ensemble. This does not mean that the risk of ignition is necessarily altered—indeed many European airports exceeded this threshold regularly even before the historical period considered here—but it points to an inevitable rethink of future storage and handling regulations, with associated economic and time budget increases.

From an HVAC—heating ventilation and air conditioning—perspective, cooling and heating requirements increase and decrease, respectively. Using the metric of 'degree days', cooling is up to approximately four times larger than heating for continental sites and comparable for oceanic ones. The wider literature is in agreement with this observation and notes that the uptake of sustainable cooling systems going forward is likely to be hampered by the more complex technological requirements which are inherent in cooling systems, as contrasted with heating. For both heating and cooling projections, the future inter-model variability is significant. This provides an infrastructure planning challenge due to the wide range of possible energy demand futures.

In terms of sustained extreme heat above a given threshold, heatwave occurrences increase markedly, approaching 10 times that observed historically. When using a threshold of 95% of the historical distribution and a minimum duration of three days, the future absolute number of heatwaves is broadly independent of the site considered, although the numbers are somewhat higher for continental sites due to the lower heat capacity of the land surrounding them compared to the oceanic and Mediterranean sites. We have not considered heatwave duration as an evolving metric in this work, but we encourage its evaluation in future studies, particularly with reference to the change in statistical distribution of daily values discussed below. For some sites, the number of heatwaves actually decreases. This is not to say that the overall heat intensity is not expected to rise—we have seen this time and again in previous results—but it does point to a fundamental change in the distribution of daily temperature values.

Much of the above discussion can be encapsulated by considering the distributional characteristics introduced by the heatwave results, which are further expounded upon by consideration of percentiles and Gaussian kernel density estimators, KDEs. Some sites are projected to move from unimodal—single peak—to bimodal temperature distributions as well as being significantly more variable around their respective average values. These combined perturbed characteristics will have compounding effects on structural (steel, concrete) and infrastructural elements (e.g., electrical installations) in terminal buildings and are also likely to exacerbate the socio-environmental and economic implications of climate change on European airport operations in the coming decades.

There is much further work to be performed in this area, and it is clear from this work—and from previous studies using the present dataset [19,20]—that the effects of climate change on European airports are multifaceted and subject to significant uncertainty going forward. It is affecting how aircraft themselves function, how urban planners consider changing local-population impacts, and even how infrastructure planning and ground staff wellbeing can be improved.

Extensions of this, and related studies, to other regions and the combining of the raw data ingestion and bias correction stages would greatly assist policymakers and stakeholders across the aviation industry. In fact, the data and methods to do so are already openly and freely available and can be installed, processed and run on a laptop. We particularly encourage studies reflecting the needs of—and impacts on—populations from the Global South, which have been historically under-represented in climate research fora.

Author Contributions: Conceptualization, J.W., P.D.W. and M.V.; methodology, J.W. and P.D.W.; software, J.W. and M.V.; validation, J.W., M.V. and P.D.W.; formal analysis, J.W., P.D.W. and M.V.; investigation, J.W., P.D.W. and M.V.; resources, J.W., P.D.W. and M.V.; data curation, J.W. and M.V.; writing, J.W. and P.D.W.; visualization, J.W.; supervision, P.D.W.; project administration, P.D.W.; funding acquisition, P.D.W. All authors have read and agreed to the published version of the manuscript.

Funding: This work is part of the AEROPLANE project, which is supported by the SESAR 3 Joint Undertaking and its founding members, Grant Agreement ID 101114682, <https://cordis.europa.eu/project/id/101114682>, accessed on 8 December 2025.

Data Availability Statement: The raw data presented in the study are openly available in the Earth System Grid Federation—ESGF—repository [21].

Acknowledgments: We thank the World Climate Research Programme (WCRP), which, through its Working Group on Coupled Modelling, coordinated and promoted CMIP6. We acknowledge the climate modelling groups for generating and making available their model output, the Earth System Grid Federation (ESGF) for archiving the data and providing access, and the many funding agencies who support the vital work of CMIP and the ESGF. We also acknowledge the computational services provided by the University of Reading’s Academic Computing Cluster (RACC) and associated research software engineering staff.

Conflicts of Interest: Author Marco Venturini was employed by the company Amigo s.r.l. The remaining authors declare that the research was conducted in the absence of any commercial or financial relationships that could be construed as a potential conflict of interest.

Abbreviations

The following abbreviations are used in this manuscript:

CDD	Cooling Degree Days
CET	Central England Temperature
CMIP6	Coupled Model Intercomparison Project (Phase 6)
ESGF	Earth System Grid Federation

HDD	Heating Degree Days
HVAC	Heating Ventilation and Air Conditioning
IATA	International Air Transport Association
ICAO	International Civil Aviation Organization
IEA	International Energy Agency
IPCC	Intergovernmental Panel on Climate Change
JJA	June–July–August
KDE	Kernel Density Estimate
SSP	Shared Socioeconomic Pathway
UTC	Coordinated Universal Time
UTCI	Universal Thermal Climate Index
WBGT	Wet Bulb Globe Temperature
WCRP	World Climate Research Programme

Appendix A. Wind Considerations

The majority of the metrics discussed in this work use so-called ‘dry bulb’ temperature values. This is simply due to the kinetic energy of the air molecules and does not take into account apparent heating or cooling due to radiative and evaporative effects nor wind. For reference, we have plotted the midday UTC 10 m wind speed magnitude for the 1st of each month at each of the 30 airports considered in this work in Figure A1. The data shown is monthly mean data from the ERA5 reanalysis product, available freely from <https://cds.climate.copernicus.eu/datasets/reanalysis-era5-single-levels-monthly-means> (accessed on 28 January 2026).

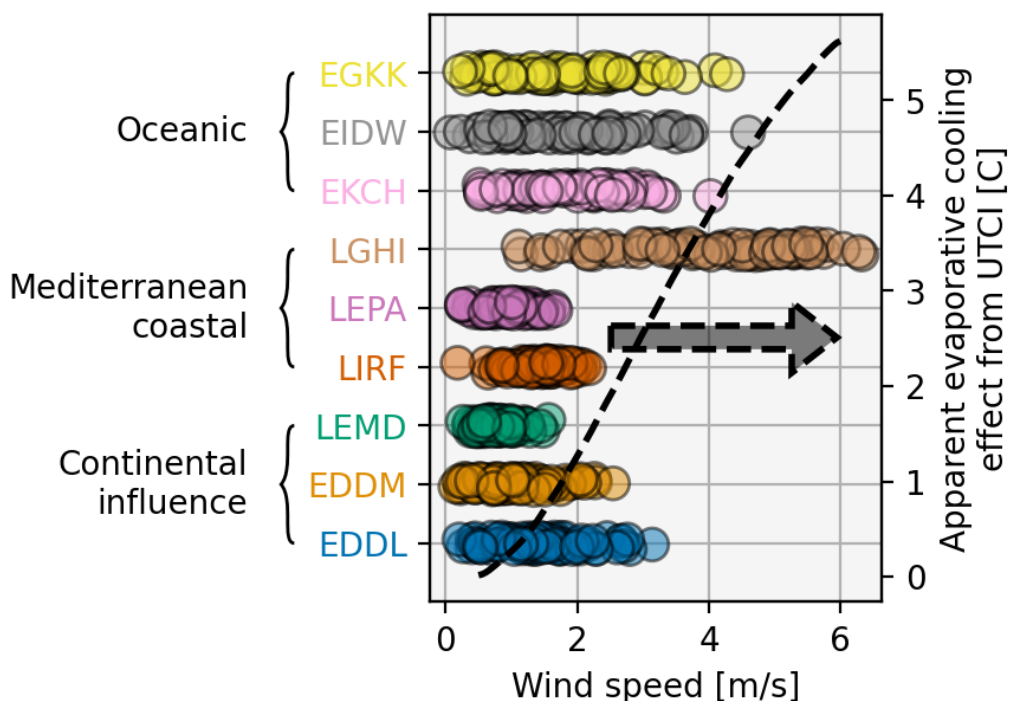


Figure A1. The monthly mean ERA5 wind speed magnitude at 10 m above ground for the airports (and climate regimes) shown on the left-hand y -axis. Some sites’ precise locations correspond to ocean points and for these the nearest land point’s value is given. The evaporative cooling effect contained within the Universal Thermal Climate Index is shown on the right-hand y -axis [26], calculated using the `pythermalcomfort` software package (version 3.8.0) described in Tartarini and Schiavon [60].

Although we do not explicitly consider the evaporative cooling effect as is included in UTCI, this is not because it is considered negligible, but rather due to the absence of

reliable, bias-corrected wind data in the present data set. These data are available as raw output from the climate models themselves, however they were not subject to the detailed analysis detailed in Trentini et al. [61]. Future extensions to this work explicitly considering wind are encouraged.

References

1. Termeer, C.J.A.M.; Dewulf, A.; Biesbroek, R. A critical assessment of the wicked problem concept: relevance and usefulness for policy science and practice. *Policy Soc.* **2019**, *38*, 167–179. <https://doi.org/10.1080/14494035.2019.1617971>.
2. Sun, Z.; Yang, H. The Wicked Problem of Climate Change: A New Approach Based on Social Mess and Fragmentation. *Sustainability* **2016**, *8*, 1312. <https://doi.org/10.3390/su8121312>.
3. Irvine, E.A.; Shine, K.P.; Stringer, M.A. What are the implications of climate change for trans-Atlantic aircraft routing and flight time? *Transp. Res. Part D Transp. Environ.* **2016**, *47*, 44–53. <https://doi.org/10.1016/j.trd.2016.04.014>.
4. Padhra, A. Emissions from auxiliary power units and ground power units during intraday aircraft turnarounds at European airports. *Transp. Res. Part D Transp. Environ.* **2018**, *63*, 433–444. <https://doi.org/10.1016/j.trd.2018.06.015>.
5. Ashley, X.M. How Airport Construction will Evolve with the Increased Effects of Climate Change. *Beyond Undergrad. Res. J.* **2019**, *3*, 5.
6. Alahmad, B.; Isachsen, I.; Alwadi, Y.; Taha, H.; Bernheim, A.; Cooke, E.; Wesley, E.; Kats, G.; Spengler, J.D. A modeling study of cool surfaces and outdoor workers productivity at San Francisco International Airport. *PNAS Nexus* **2025**, *4*, pgae593. <https://doi.org/10.1093/pnasnexus/pgae593>.
7. Burbidge, R.; Paling, C.; Dunk, R.M. A systematic review of adaption to climate change impacts in the aviation sector. *Transp. Rev.* **2024**, *44*, 8–33. <https://doi.org/10.1080/01441647.2023.2220917>.
8. Deshayes, T.A.; Hsouna, H.; Braham, M.A.A.; Arvisais, D.; Pageaux, B.; Ouellet, C.; Jay, O.; Maso, F.D.; Begon, M.; Saidi, A.; Gendron, P.; et al. Work–rest regimens for work in hot environments: A scoping review. *Am. J. Ind. Med.* **2024**, *67*, e23569. <https://doi.org/10.1002/ajim.23569>.
9. Torbat Esfahani, M.; Awolusi, I.; Hatipkarasulu, Y. Heat Stress Prevention in Construction: A Systematic Review and Meta-Analysis of Risk Factors and Control Strategies. *Int. J. Environ. Res. Public Health* **2024**, *21*, 1681. <https://doi.org/10.3390/ijerph21121681>.
10. Spector, J.T.; Masuda, Y.J.; Wolff, N.H.; Calkins, M.; Seixas, N.S. Heat Exposure and Occupational Injuries: Review of the Literature and Implications. *Curr. Environ. Health Rep.* **2019**, *6*, 286–296. <https://doi.org/10.1007/s40572-019-00250-8>.
11. Zhao, M.; Lee, J.K.W.; Kjellstrom, T.; Cai, W. Assessment of the economic impact of heat-related labor productivity loss: a systematic review. *Clim. Change* **2021**, *167*, 31. <https://doi.org/10.1007/s10584-021-03160-7>.
12. Sun, Y.; Zhu, S.; Wang, D.; Duan, J.; Lu, H.; Yin, H.; Tan, C.; Zhang, L.; Zhao, M.; Cai, W.; et al. Global supply chains amplify economic costs of future extreme heat risk. *Nature* **2024**, *631*, 123–130. <https://doi.org/10.1038/s41586-024-07147-z>.
13. Hasegawa, T.; Fujimori, S.; Havlík, P.; Valin, H.; Leclère, B.; Riahi, K.; Havlík, P. Quantifying the Economic Impact of Changes in Energy Demand for Space Heating and Cooling. *Palgrave Commun.* **2016**, *2*, 16013. <https://doi.org/10.1057/palcomms.2016.13>.
14. Lizana, J.; Miranda, N.D.; Gross, L.; Mazzone, A.; Cohen, F.; Palafox-Alcantar, G.; Fahr, P.; Jani, A.; Renaldi, R.; McCulloch, M.; et al. Overcoming the Incumbency and Barriers to Sustainable Cooling. *Build. Cities* **2023**, *4*, 1075–1097. <https://doi.org/10.5334/bc.255>.
15. Liu, Q.; Fu, C.; Xu, Z.; Ding, A. Global warming intensifies extreme day-to-day temperature changes in mid–low latitudes. *Nat. Clim. Change* **2025**, *16*, 69–76. <https://doi.org/10.1038/s41558-025-02486-9>.
16. Palu, R.; Mahmoud, H. Impact of climate change on the integrity of the superstructure of deteriorated U.S. bridges. *PLoS ONE* **2019**, *14*, e0223307.
17. Grose, T.K. Hot & Bothered. In *ASEE Prism*; American Society for Engineering Education: Washington, DC, USA, 2022.
18. Barbi, S.R.; Labi, S.; Roesler, J.R. Incorporating Climate Change Effects in Airport Pavement Design and Management. *Transp. Res. Rec.* **2023**, *2677*, 118–136. <https://doi.org/10.1177/03611981231155909>.
19. Williams, J.; Williams, P.D.; Guerrini, F.; Venturini, M. Quantifying the Effects of Climate Change on Aircraft Take-Off Performance at European Airports. *Aerospace* **2025**, *12*, 165. <https://doi.org/10.3390/aerospace12030165>.
20. Williams, J.; Williams, P.D.; Venturini, M.; Padhra, A.; Gratton, G.; Rapsomanikis, S. The Impacts of Climate Change on Aircraft Noise near European Airports. *Aerospace* **2025**, *12*, 815. <https://doi.org/10.3390/aerospace12090815>.
21. Eyring, V.; Bony, S.; Meehl, G.A.; Senior, C.A.; Stevens, B.; Stouffer, R.J.; Taylor, K.E. Overview of the Coupled Model Intercomparison Project Phase 6 (CMIP6) Experimental Design and Organization. *Geosci. Model Dev.* **2016**, *9*, 1937–1958. <https://doi.org/10.5194/gmd-9-1937-2016>.
22. Cinquini, L.; Crichton, D.; Mattmann, C.; Harney, J.; Shipman, G.; Wang, F.; Ananthakrishnan, R.; Miller, N.; Denvil, S.; Morgan, M.; et al. The Earth System Grid Federation: An open infrastructure for access to distributed geospatial data. *Future Gener. Comput. Syst.* **2014**, *36*, 400–417. <https://doi.org/10.1016/j.future.2013.07.002>.

23. van Vuuren, D.P.; Riahi, K.; Calvin, K.V.; Dellink, R.; Emmerling, J.; Fujimori, S.; KC, S.; Kriegler, E.; O'Neill, B.C. The Shared Socio-economic Pathways: Trajectories for human development and global environmental change. *Glob. Environ. Change* **2017**, *42*, 267–281. <https://doi.org/10.1016/j.gloenvcha.2016.10.009>.

24. Ahmed, M.; Seraj, R.; Islam, S.M.S. The k-Means Algorithm: A Comprehensive Survey and Performance Evaluation. *Electronics* **2020**, *9*, 1295. <https://doi.org/10.3390/electronics9081295>.

25. Peel, M.C.; Finlayson, B.L.; McMahon, T.A. Updated world map of the Köppen-Geiger climate classification. *Hydrol. Earth Syst. Sci.* **2007**, *11*, 1633–1644. <https://doi.org/10.5194/hess-11-1633-2007>.

26. Błażejczyk, K.; Jendritzky, G.; Bröde, P.; Fiala, D.; Havenith, G.; Epstein, Y.; Psikuta, A.; Kampmann, B. An introduction to the Universal Thermal Climate Index (UTCI). *Geogr. Pol.* **2013**, *86*, 5–10. <https://doi.org/10.7163/GPol.2013.1>.

27. Brimicombe, C.; Lo, C.H.B.; Pappenberger, F.; Di Napoli, C.; Maciel, P.; Quintino, T.; Cornforth, R.; Cloke, H.L. Wet Bulb Globe Temperature: Indicating Extreme Heat Risk on a Global Grid. *GeoHealth* **2023**, *7*, e2022GH000701. <https://doi.org/10.1029/2022GH000701>.

28. Chesnoiu, G.; Chiapello, I.; Ferlay, N.; Nabat, P.; Mallet, M.; Riffault, V. Regional modeling of surface solar radiation, aerosol, and cloud cover spatial variability and projections over northern France and Benelux. *Atmos. Chem. Phys.* **2025**, *25*, 1307–1331. <https://doi.org/10.5194/acp-25-1307-2025>.

29. Masterton, J.M.; Richardson, F.A. *Humidex: A Method of Quantifying Human Discomfort Due to Excessive Heat and Humidity*; Technical Report En57-23/1; Atmospheric Environment Service, Environment Canada: Downsview, ON, Canada, 1979.

30. Wallace, J.M.; Hobbs, P.V. *Atmospheric Science: An Introductory Survey*, 2nd ed.; Elsevier Academic Press: Amsterdam, The Netherlands, 2006.

31. IEC 60079-10-1 3.0 edition; Explosive Atmospheres—Part 10-1: Classification of Areas—Explosive Gas Atmospheres. International Electrotechnical Commission: Geneva, Switzerland, 2020.

32. Petri, Y.; Caldeira, K. Impacts of global warming on residential heating and cooling degree-days in the United States. *Sci. Rep.* **2015**, *5*, 12427. <https://doi.org/10.1038/srep12427>.

33. Harvey, L.D. Using modified multiple heating-degree-day (HDD) and cooling-degree-day (CDD) indices to estimate building heating and cooling loads. *Energy Build.* **2020**, *229*, 110475. <https://doi.org/10.1016/j.enbuild.2020.110475>.

34. Ramon, D.; Allacker, K.; De Troyer, F.; Wouters, H.; van Lipzig, N.P. Future heating and cooling degree days for Belgium under a high-end climate change scenario. *Energy Build.* **2020**, *216*, 109935. <https://doi.org/10.1016/j.enbuild.2020.109935>.

35. Miranda, N.D.; Lizana, J.; Sparrow, S.N.; Zachau-Walker, M.; Watson, P.A.G.; Wallom, D.C.H.; Khosla, R.; McCulloch, M. Change in cooling degree days with global mean temperature rise increasing from 1.5 °C to 2.0 °C. *Nat. Sustain.* **2023**, *6*, 1326–1330. <https://doi.org/10.1038/s41893-023-01155-z>.

36. Deroubaix, A.; Labuhn, I.; Camredon, M.; Gaubert, B.; Monerie, Pa.; Popp, M.; Ramarohetra, J.; Ruprich-Robert, Y.; Silvers, L.G.; Siour, G. Large Uncertainties in Trends of Energy Demand for Heating and Cooling Under Climate Change. *Nat. Commun.* **2021**, *12*, 25504. <https://doi.org/10.1038/s41467-021-25504-8>.

37. Perkins, S.E.; Alexander, L.V. On the Measurement of Heat Waves. *J. Clim.* **2013**, *26*, 4500–4517. <https://doi.org/10.1175/JCLI-D-12-00383.1>.

38. Bunting, W.; Tolmanov, V.; Keellings, D. What is a heat wave: A survey and literature synthesis of heat wave definitions across the United States. *PLoS Clim.* **2024**, *3*, e0000468. <https://doi.org/10.1371/journal.pclm.0000468>.

39. Zhao, J.J.; Leyva, E.W.; Wong, K.A.; Kataoka-Yahiro, M.; Saligan, L.N. Heat Stress and Determinants of Kidney Health Among Agricultural Workers in the United States: An Integrative Review. *Int. J. Environ. Res. Public Health* **2025**, *22*, 1268. <https://doi.org/10.3390/ijerph22081268>.

40. Rifkin, D.I.; Long, M.W.; Perry, M.J. Climate change and sleep: A systematic review of the literature and conceptual framework. *Sleep Med. Rev.* **2018**, *42*, 3–9. <https://doi.org/10.1016/j.smrv.2018.07.007>.

41. Habibi, P.; Razmjouei, J.; Moradi, A.; Mahdavi, F.; Fallah-Aliabadi, S.; Heydari, A. Climate change and heat stress resilient outdoor workers: findings from systematic literature review. *BMC Public Health* **2024**, *24*, 19212. <https://doi.org/10.1186/s12889-024-19212-3>.

42. Molina, M.O.; Soares, P.M.M.; Lima, M.M.; et al. Updated insights on climate change-driven temperature variability across historical and future periods. *Clim. Change* **2025**, *178*, 97. <https://doi.org/10.1007/s10584-025-03937-0>.

43. Saifudeen, A.; Mani, M. Adaptation of Buildings to Climate Change: An Overview. *Front. Built Environ.* **2024**, *10*, 1327747. <https://doi.org/10.3389/fbuil.2024.1327747>.

44. Yang, R.; Zhan, C.; Sun, L.; Shi, C.; Fan, Y.; Wu, Y.; Yang, J.; Liu, H. Modelling the reflective cracking features of asphalt overlay for airport runway under temperature and airplane load coupling factors. *Constr. Build. Mater.* **2024**, *403*, 138774. <https://doi.org/10.1016/j.conbuildmat.2024.138774>.

45. Hourdin, F.; Mauritsen, T.; Gettelman, A.; Golaz, J.C.; Balaji, V.; Duan, Q.; Folini, D.; Ji, D.; Klocke, D.; Qian, Y.; et al. The Art and Science of Climate Model Tuning. *Bull. Am. Meteorol. Soc.* **2017**, *98*, 589–602. <https://doi.org/10.1175/BAMS-D-15-00135.1>.

46. Burt, S. Evaluation and verification of new UK air temperature extremes during the July 2022 heatwave. Part 1: maximum temperatures. *Weather* **2025**, *80*, 70–78. <https://doi.org/10.1002/wea.7709>.

47. Nazarenko, L.S.; Tausnev, N.; Russell, G.L.; Rind, D.; Miller, R.L.; Schmidt, G.A.; Bauer, S.E.; Kelley, M.; Ruedy, R.; Ackerman, A.S.; et al. Future Climate Change Under SSP Emission Scenarios with GISS-E2.1. *J. Adv. Model. Earth Syst.* **2022**, *14*, e2021MS002871. <https://doi.org/10.1029/2021MS002871>.

48. Tollefson, J. Earth breaches 1.5 °C climate limit for the first time: what does it mean? *Nature* **2025**, *625*, 10–11. <https://doi.org/10.1038/d41586-025-00010-9>.

49. Mehmood, A.; Amber, K.P.; Usman, M.; Friedrich, D. Integrating Latent Load into the Cooling Degree Days Concept. *Buildings* **2024**, *14*, 106. <https://doi.org/10.3390/buildings14010106>.

50. Cao, J.; Li, M.; Zhang, R.; Wang, M. An efficient climate index for reflecting cooling energy consumption: Cooling degree days based on wet bulb temperature. *Meteorol. Appl.* **2021**, *28*, e2005. <https://doi.org/10.1002/met.2005>.

51. Bhatnagar, M. Determining base temperature for heating and cooling degree-days for India. *J. Build. Eng.* **2018**, *18*, 293–304. <https://doi.org/10.1016/j.jobe.2018.03.020>.

52. Parker, D.E.; Legg, T.P.; Folland, C.K. A new daily Central England Temperature Series, 1772–1991. *Int. J. Climatol.* **1992**, *12*, 317–342. <https://doi.org/10.1002/joc.3370120402>.

53. Seneviratne, S.I.; Corti, T.; Davin, E.L.; Hirschi, M.; Jaeger, E.B.; Lehner, I.; Orlowsky, B.; Teuling, A.J. Investigating soil moisture–climate interactions in a changing climate: A review. *Earth-Sci. Rev.* **2010**, *99*, 125–161. <https://doi.org/10.1016/j.earscirev.2010.02.004>.

54. Liu, J.; Qi, J.; Yin, P.; Liu, W.; He, C.; Gao, Y.; Zhou, L.; Zhu, Y.; Kan, H.; Chen, R.; et al. Rising cause-specific mortality risk and burden of compound heatwaves amid climate change. *Nat. Clim. Change* **2024**, *14*. <https://doi.org/10.1038/s41558-024-02137-5>.

55. IEA. Climate Resilience—Power Systems in Transition. Licence: CC BY 4.0. 2020. Available online: <https://www.iea.org/reports/power-systems-in-transition/climate-resilience> (accessed on 28 January 2026).

56. Croce, P.; Formichi, P.; Landi, F. Climate Change: Impacts on Climatic Actions and Structural Reliability. *Appl. Sci.* **2019**, *9*, 5416. <https://doi.org/10.3390/app9245416>.

57. Voskaki, A.; Budd, L.; Mason, K. The impact of climate hazards to airport systems: a synthesis of the implications and risk mitigation trends. *Transp. Rev.* **2023**, *43*, 216–239. <https://doi.org/10.1080/01441647.2022.2163319>.

58. Williams, P.D. Increased light, moderate, and severe clear-air turbulence in response to climate change. *Adv. Atmos. Sci.* **2017**, *34*, 576–586. <https://doi.org/10.1007/s00376-017-6268-2>.

59. Singh, D.K.; Sanyal, S.; Wuebbles, D.J. Understanding the role of contrails and contrail cirrus in climate change: A global perspective. *Atmos. Chem. Phys.* **2024**, *24*, 9219–9262. <https://doi.org/10.5194/acp-24-9219-2024>.

60. Tartarini, F.; Schiavon, S. pythermalcomfort: A Python package for thermal comfort research. *SoftwareX* **2020**, *12*, 100578. <https://doi.org/10.1016/j.softx.2020.100578>.

61. Trentini, L.; Venturini, M.; Guerrini, F.; Gesso, S.D.; Calmanti, S.; Petitta, M. Identifying Climate Extremes in Southern Africa through Advanced Bias Correction of Climate Projections. *Bull. Atmos. Sci. Technol.* **2025**, *6*, 9. <https://doi.org/10.1007/s42865-025-00097-y>.

Disclaimer/Publisher’s Note: The statements, opinions and data contained in all publications are solely those of the individual author(s) and contributor(s) and not of MDPI and/or the editor(s). MDPI and/or the editor(s) disclaim responsibility for any injury to people or property resulting from any ideas, methods, instructions or products referred to in the content.